

Threshold of Detection of Diffuse Lung Disease

Peter Chicco, John S. Magnussen, Amanda W. Palmer, Douglas W. Mackey and Hans Van der Wall

Graduate School of Biomedical Engineering, University of New South Wales; Department of Nuclear Medicine, Concord Hospital; and Department of Radiology, St. George Hospital, Sydney, Australia

A scintigraphic model of the lungs was used to study the threshold of detection of diffuse disease of the lungs. **Methods:** Randomly distributed cold lesions of 4, 8, 12 and 16 mm³ block sizes were created, occupying 0%–50% of lung tissue in steps of 1%. These were submitted for reporting to five observers each with a normal study for comparison. **Results:** No observer detected lesions of 4-mm³ block size even when up to 50% of the lung was involved. All observers detected lesions of 8-mm³ block size when a mean of 27% of lung tissue was involved with lesions. As lesion size increased to 12 and 16 mm³, observers detected lesions when a mean of 10% and 6% of lung tissue was involved, respectively. Comparison between views for each observer showed that the lateral and anterior oblique views were used more often than the anterior, posterior oblique and posterior views. **Conclusion:** This model suggests that pulmonary scintigraphy has the potential to detect a diffuse disease such as emphysema at an early stage of lung involvement. In general, small anatomic lesions appear to have more profound scintigraphic consequences. However, even scintigraphic lesions of the order of size of the pulmonary acinus are easily detected.

Key Words: Monte Carlo simulation; lung scintigraphy; perception; emphysema

J Nucl Med 1999; 40:85–90

Emphysema is a common clinical condition that causes a significant degree of morbidity (1). There has been a concerted attempt to detect the condition at a preclinical stage to prevent progression of the disease to eventual end-stage lung failure. Numerous modalities have been adopted, ranging from pulmonary function testing to plain radiography and high-resolution CT. The plethora of investigations is a marker of the inability to find a single valid method of assessment; although they have been shown to be promising, few careful studies have examined the possibility of early detection using nuclear medicine techniques. One study found the technique of tomographic perfusion scintigraphy to be more sensitive than high-resolution CT in an animal model of early emphysema (2).

A major problem in studying the potential of scintigraphy to demonstrate early disease is the lack of a true “gold standard” by which to judge its performance. Fundamental to the problem is the need to establish the threshold and

absolute minimum lesion size that can be detected. To explore these problems with certainty, a model of the scintigraphic anatomy of the lungs was constructed and used to overcome the problems encountered with clinical studies and physical phantoms. This allowed precise determination of lesion size and placement in a model that was indistinguishable from clinical images of the lungs.

The aims of the study were to determine the threshold of detection of cold lesions that varied in size and density and the optimal views of the lungs in which these abnormalities were best perceived.

MATERIALS AND METHODS

The phantom used in the construction of the model for this study was based on CT data from a supine man of height 178 cm, weighing 70 kg (3), who was chosen for his similarity to the dosimetry standard mathematical phantom (4).

The Monte Carlo simulation package used for this work was the Photon History Generator (5,6), which models the emission, scatter and attenuation of photons in a heterogeneous phantom, followed by the photons' subsequent collimation and detection. All simulations were performed on an Intel-based platform and required approximately 76 h each to complete.

Simulations were performed for a 23.6-mm-thick parallel-hole collimator, using a 32.5-cm radius of rotation and with a system full width at half maximum (FWHM) of 12.5 mm. The isotope modeled was ^{99m}Tc, collected with a symmetric 20% energy window centered around 140 keV into a 256 × 256 matrix, resulting in counts of 600–700 k per view when no defects were present. The views collected were anterior, posterior, both laterals, anterior obliques and posterior obliques.

A series of studies was performed in four groups, distinguished by the size of individual defects present. Defects in groups 1–4 were 4, 8, 12 and 16 mm³, respectively (Fig. 1). These were distributed uniformly throughout both lungs in a random manner. Within each group, the amount of lung tissue involved in defects varied from 0% (normal) up to 50% in steps of 1%, giving 51 studies in each group.

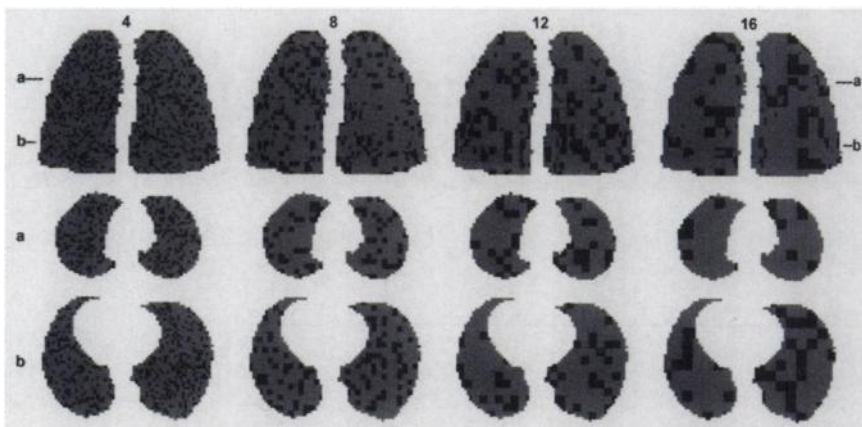
The number of individual defects in both lungs in a study was related to the total amount of lung tissue involved and the size of each defect. For example, 64 times as many 4-mm³ defects as 16 mm³ were required to involve the same amount of the lung tissue. Thus, there were 51 studies per group and 204 studies in total. Once completed, the studies were placed in random order before reporting.

Studies were reviewed by five observers, two of whom had more than 10 y of nuclear medicine experience, and the remainder by resident staff with less than 2 y of experience. All observers independently considered them suitable for diagnostic purposes.

Received Nov. 17, 1997; revision accepted Apr. 19, 1998.

For correspondence or reprints contact: John S. Magnussen, MB, BS, FRSM, Department of Nuclear Medicine, Concord Hospital, Hospital Rd., Concord, NSW, 2139, Australia.

FIGURE 1. Schematic representation of lesions defined in model before submission to Monte Carlo simulations. It demonstrates distribution of lesions of block sizes 4, 8, 12 and 16 mm³ with 25% of lung tissue involved by lesions (shown as black areas). Top row is posterior view of lungs, and lower two rows are cross sections at levels indicated. Diagrams show that lesions were uniformly distributed throughout lung tissue.



They were asked to examine the studies for the presence of any defect (a positive response), using a normal study produced from the same anatomic phantom as a reference, and a note was made of all views showing a defect. A defect was considered to be present if any difference could be discerned between the study and the normal by the observer, and a yes/no response was required. All reporting was performed independently, under identical conditions on a computer screen, on three separate occasions to reduce the effects of fatigue.

The threshold for detection was defined as the minimum percentage of lung tissue involved by lesions for an abnormality to be detected. Results were ordered by the size and proportion of lung tissue occupied by lesions. A threshold for each observer was calculated by the weighted average of the range between the first positive and the last negative response.

Optimal views for the detection of lesions were determined for each observer. These were calculated as a proportion for each view out of the total number of positive responses. A comparison of these proportions using a χ^2 significance test of a 2×8 contingency table

was performed. The null hypothesis was that all eight views were used equally.

For each observer, comparisons between views were performed using a comparison of two proportions, for the unpaired case. The null hypothesis was that the proportion for each view was no different from that of any other view. All possible combinations of views were considered.

RESULTS

No defects of block size 4 mm³ could be seen in lesions involving up to 50% of the lung (Fig. 2). For lesions of 8-mm³ block size, all observers detected an abnormality when lesions occupied a group mean of 27% of lung tissue. In the case of the 12- and 16-mm³ block sizes, an abnormality was detected when the group mean of lung tissue occupied by lesions decreased to 10% and 6%, respectively. Examples of when all observers identified discrete lesions in such studies are shown in Figures 3 and 4, whereas Figure 5

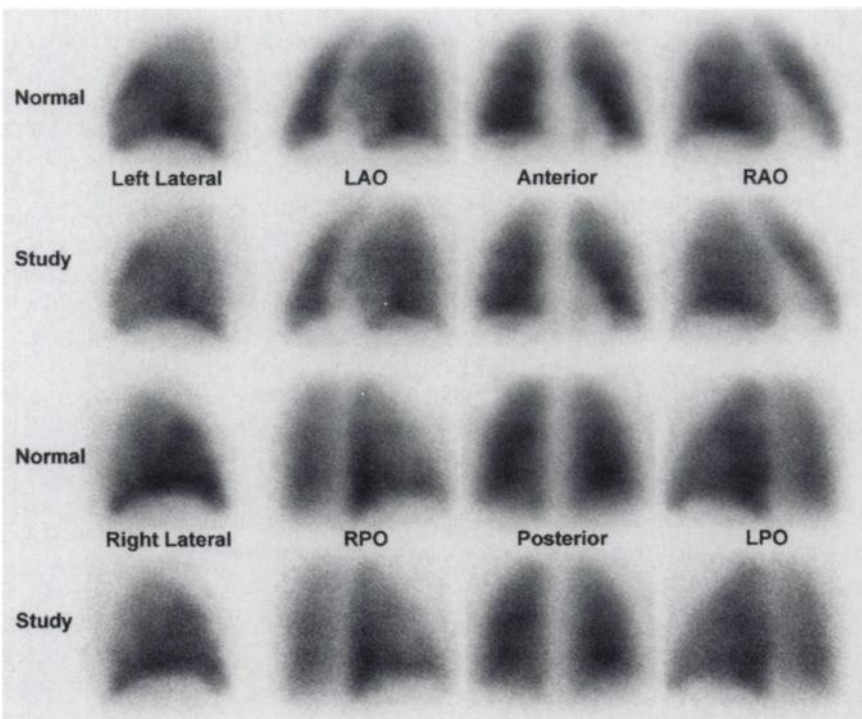


FIGURE 2. Lung scan in eight standard views of 4-mm³ block sizes involving 50% of lung tissue. In comparison to the normal study, this study appears "noisy," but no discrete lesions were identified by any observers.

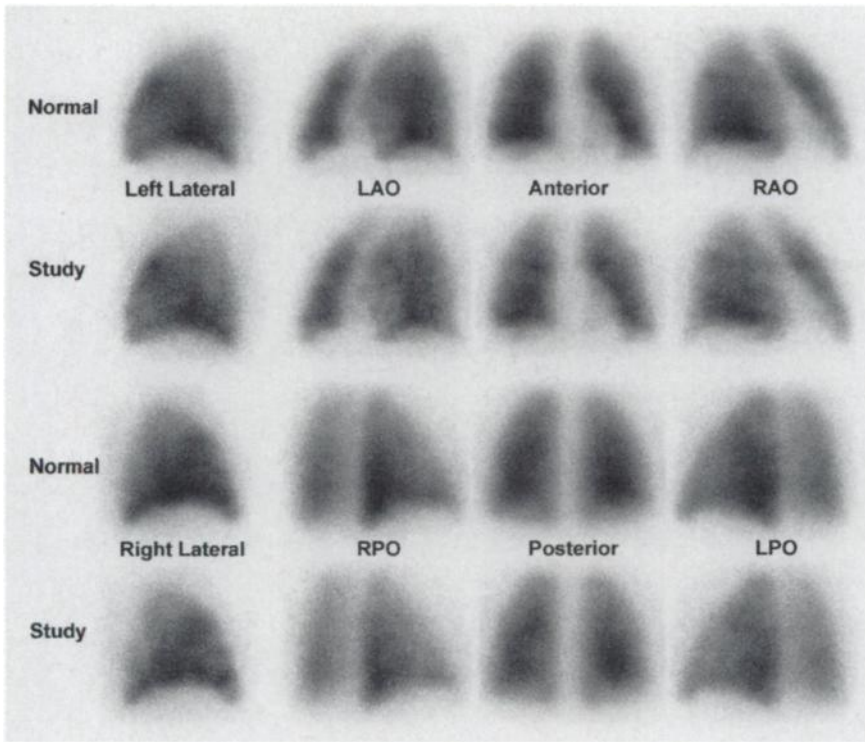


FIGURE 3. Lung scan in eight standard views of 8-mm³ block sizes involving 42% of lung tissue. In comparison to normal study, this study was identified as containing multiple lesions by all observers.

shows a comparison with a patient study. A more detailed analysis of these results is shown in Table 1. As the lesion size increased, the threshold for detection for each person and the mean value for the group of observers decreased. There was a smaller decrease seen in the SEM.

For each observer, the χ^2 test of significance with 8-1 degrees of freedom showed that there was a significant

departure from the null hypothesis ($P < 0.0001$). Thus all eight views were not used equally when reviewed by observers. Table 2 shows the eight views, ordered by their relative frequency of use, when averaged for all five observers.

Comparison between views for each observer showed that the lateral and anterior oblique views were used significantly

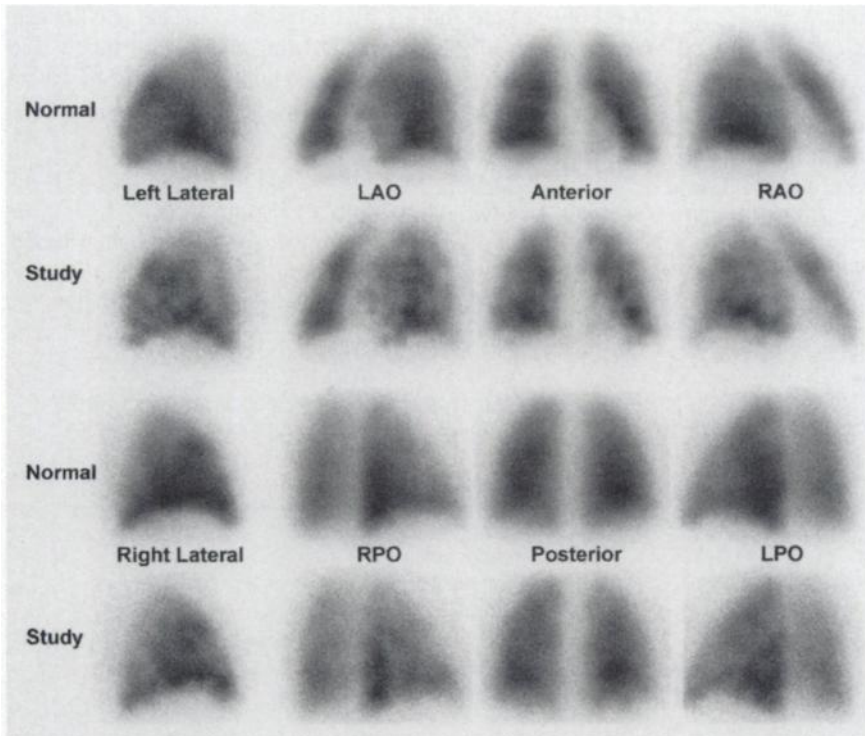


FIGURE 4. Lung scan in eight standard views of 16-mm³ block sizes involving 40% of lung tissue. In comparison to normal study, this study was identified as containing multiple lesions by all observers.

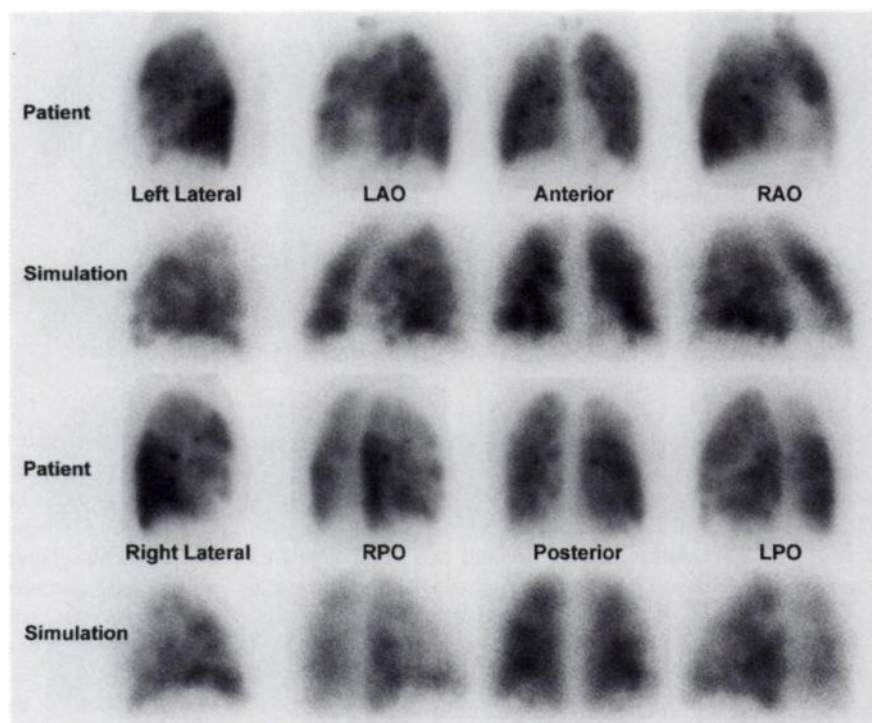


FIGURE 5. Shows comparison in eight standard views, between patient study and simulation selected to approximate severity of disease. In simulation, 16-mm³ block size defects involved 50% of lung tissue. Patient study was performed after ventilation with technegas, using ^{99m}Tc-MAA and triple-head camera.

more often than the anterior, posterior oblique and posterior views ($P < 0.05$). There were generally no differences demonstrable between the laterals and anterior oblique views, as was also the case with the anterior, posterior oblique and posterior views.

DISCUSSION

The model used in this study has several characteristics that make it a valuable tool in such investigations. It allows absolute accuracy about the size, placement and density of lesions introduced into the image. Just as important, it provides the eight "standard" views used in pulmonary scintigraphy with a similar number of counts per study and the expected scatter and attenuation characteristics of a clinical study. These qualities cannot be reproduced in a clinical study with certainty, because there is no clinical

"gold standard" available to ensure accuracy. In this instance the model allowed manipulation of lesion size, which varied from 4 to 16-mm³ blocks of absent activity (Fig. 1), as well as the density of the lesions throughout both lungs. In this way, the percentage of counts replaced by the introduction of the lesions could be quantitated as well.

The FWHM of the line spread function of the gamma camera system used in this model is 12.5 mm. It means that lesions would need to be between 6 and 9 mm³ to reach a threshold of detectability by observers (7). This was indeed the case with all observers detecting the 8-mm³ block size lesions. No observer was able to detect the 4-mm³ block size lesions, which were well below the gamma camera system resolution.

Just as important as absolute lesion size is the issue of contrast. Lesions were held constant at 4-, 8-, 12- or 16-mm³ blocks, with the number of lesions distributed diffusely through the lungs being varied. For the 8-mm³ blocks, it required lesions to occupy an average of 27% of

TABLE 1
Threshold of Detection for Each Observer

Observer	Threshold (%)		
	8 mm ³	12 mm ³	16 mm ³
1	33	12	8
2	27	8	7
3	28	10	7
4	23	9	4
5	25	10	6
Mean	27	10	6
SEM	2	1	1

Threshold of detection = minimum percentage of lung tissue involved by lesions for an abnormality to be detected.

TABLE 2
Average Percentage of Times Each View was Used in Detection of a Lesion, for All Five Observers

View	Percentage
Left lateral	90
Left anterior oblique	88
Right anterior oblique	86
Right lateral	85
Anterior	75
Left posterior oblique	69
Right posterior oblique	60
Posterior	53

lung counts before the study was reported as abnormal. As the lesion sizes increased further to 12- and 16-mm³ blocks, the threshold of detection of lesions decreased to 10% and 6% of the lung counts occupied by lesions, respectively. Notably, no perceptible abnormalities were reported with 4-mm³ block lesions, even when such lesions accounted for 50% of the counts in the lungs (Fig. 2).

Most observers detected the diffuse defects best in the left lateral and left anterior oblique projections, followed by the right anterior oblique and right lateral projections. The preference for the left-sided views may reflect the greater density of lung tissue in the base of the right lung, where there is a radial arrangement of two rows of segments. In comparison, there is one row of segments arranged around the cardiac impression for the left lung base. Thus lesions in the base of the left lung would be detected with less lung involvement, because the background number of counts would be less than on the right side, improving the lesion-to-background ratio.

These findings have implications for emphysema in the clinical setting. Emphysema is a common disease that medical imaging has not been able to address adequately, particularly at a nascent stage. It is especially prevalent in smokers, although one autopsy series found a general prevalence of 50%, which increased to 73% if minimal disease was included (1). In terms of pathophysiology, the disease is characterized by various patterns of permanent airspace destruction and enlargement, without significant fibrosis (8). These changes are manifest clinically as loss of lung elasticity and radiologically as reduced tissue density and attenuation of vascular markings. Attempts have been made to detect the disease at an early stage by the use of pulmonary function testing, plain chest radiography, CT and various scintigraphic techniques (9,10).

In a comprehensive review (11) of the subject, it was concluded that high-resolution CT with 1-mm collimation was more sensitive than CT collimated at 5–10 mm. Overall, CT was more sensitive than pulmonary function testing. However, the performance of CT varied with the type of emphysema, being better at detecting centrilobular disease than panacinar disease, which has a predilection for the lung bases. The scintigraphic literature is less plentiful and rigorous. One clinical study found that tomographic ventilation imaging with ^{99m}Tc technegas showed more extensive changes than high-resolution CT scanning (12). Lesions as small as 5 mm on CT scanning caused more extensive functional changes in the scintigraphic images (13,14).

More rigorous analysis of CT and scintigraphy has been undertaken in an animal model of emphysema (2). This study examined the efficacy of high-resolution CT, tomographic perfusion imaging and planar ventilation imaging with ¹³³Xe. A model of mild, histologically confirmed emphysema was assessed after instillation of elastase into the left lower lobe bronchus of pigs. Planar ventilation imaging did not detect any significant abnormalities, whereas

perfusion scintigraphy detected all abnormalities as areas of reduced perfusion. High-resolution CT detected half the lesions. It is a promising result that suggests the possibility of very early detection of the disease when intervention may prove beneficial, before irreversible, clinically apparent disease. The failure of ventilation imaging to detect an abnormality may be due to the failure to acquire a tomographic study and the nature of the agent. With ventilation studies using ¹³³Xe, "hot spots" are a marker of significant parenchymal disease, which is usually advanced and often clinically obvious. In contrast, ventilation imaging with ^{99m}Tc technegas demonstrates sites of peripheral parenchymal disease as regions of reduced activity (12). The agent also allows the acquisition of a tomographic study with relative ease. More severe central parenchymal disease may be manifested by central deposition of ^{99m}Tc technegas (15).

When this limited but rigorous scintigraphic technique is coupled to the findings of this study, it suggests that early emphysema could be detected by either perfusion or ventilation imaging. There is a clear and well-defined threshold at which an observer is capable of detecting the disease state and which may well be improved with tomographic imaging of the lungs, producing superior contrast resolution. The key to the success of the scintigraphic technique is that small, anatomically apparent lesions appear to produce far greater functional disturbances in both ventilation and perfusion studies, enhancing the likelihood of detection. The worst case situation was deliberately chosen, such that small lesions would appear with approximately the same scintigraphic dimensions as the anatomic change at the level of the acinus. The diameter of an average acinus, a unit of gas exchange, is approximately 8 mm (16), which is of the same magnitude as the smallest detectable lesion size. The results confirm that the scintigraphic manifestations of a relatively diffuse disease such as emphysema should be detected at a nascent stage.

CONCLUSION

A model of the scintigraphic anatomy of the lungs has been used to assess the threshold at which an observer detects lesions in comparison with a normal study. Because of limitations in system resolution, no lesions of 4-mm³ block size were detected, even when they occupied 50% of the lung counts. All observers detected 8-mm³ block lesions in a narrow grouping when 27% of the counts in the lung were lost. The threshold at which 12- and 16-mm³ block lesions were detected was significantly better, with loss of only 10% and 6% of lung counts, respectively. Detection of such diffuse abnormalities was best in the left lung in the lateral and anterior oblique projections, followed by the right anterior oblique and lateral views. This may reflect the complex anatomy and segmental crowding in the base of the right lung. The model suggests that scintigraphic imaging has the potential to detect emphysema at an early stage.

ACKNOWLEDGMENT

This work was supported by research grants from the Nuclear Medicine Research Foundation, Sydney, Australia.

REFERENCES

1. Thurlbeck WM. The incidence of pulmonary emphysema: with observations on the relative incidence and spatial distribution of various types of emphysema. *Am Rev Respir Dis.* 1963;87:206-215.
2. Noma S, Moskowitz GW, Herman PG, Khan A, Rojas KA. Pulmonary scintigraphy in elastase-induced emphysema in pigs. Correlation with high-resolution computed tomography and histology. *Invest Radiol.* 1992;27:429-435.
3. Zubal IG, Harrell CR, Smith EO, Rattner Z, Gindi G, Hoffer PB. Computerized three-dimensional segmented human anatomy. *Med Phys.* 1994;21:299-302.
4. Society of Nuclear Medicine. *Estimates of Specific Absorbed Fractions for Photon Sources Uniformly Distributed in Various Organs of a Heterogeneous Phantom.* New York, NY: Society of Nuclear Medicine; 1978:5.
5. Lewellen TK, Anson CP, Haynor DR, et al. Design of a simulation system for emission tomographs [abstract]. *J Nucl Med.* 1988;29:871-871.
6. Haynor DR, Harrison RL, Lewellen TK. The use of importance sampling techniques to improve the efficiency of photon tracking in emission tomography simulations. *Med Phys.* 1991;18:990-1001.
7. Sorenson JA, Phelps ME. *Physics in Nuclear Medicine.* Orlando, FL: Grune & Stratton; 1987.
8. American Thoracic Society. Chronic bronchitis, asthma and pulmonary emphysema: a statement by the Committee on Diagnostic Standards for Nontuberculous Respiratory Diseases. *Am Rev Respir Dis.* 1962;85:762-768.
9. Spouge D, Mayo JR, Cardoso W, Muller NL. Panacinar emphysema: CT and pathologic findings. *J Comput Assist Tomogr.* 1993;17:710-713.
10. Muller NL, Miller RR, Abboud RT. "Density mask" an objective method to quantitate emphysema using computed tomography. *Chest.* 1988;94:782-787.
11. Thurlbeck WM, Muller NL. Emphysema: definition, imaging, and quantification. *AJR.* 1994;163:1017-1025.
12. Satoh K, Tanabe M, Nakano S, Nishiyama Y, Takahashi K. Comparison of ^{99m}Tc -technegas scintigraphy and high resolution CT in pulmonary emphysema. *Jpn J Nucl Med.* 1995;32:487-494.
13. Murata K, Itoh H, Todo G. Centrilobular lesions of the lung: demonstrated by high-resolution CT and pathologic correlation. *Radiology.* 1986;161:641-645.
14. Webb WR, Stein MG, Finkbeiner WE, Im JG, Lynch D, Gamsu G. Normal and disease isolated lungs: high-resolution CT. *Radiology.* 1988;166:81-87.
15. James JM, Lloyd JJ, Leahy BC, et al. $^{99\text{Tcm}}$ -technegas and krypton-81m ventilation scintigraphy: a comparison in known respiratory disease. *Br J Radiol.* 1992;65:1075-1082.
16. Pump KK. Morphology of the acinus of the human lung. *Dis Chest.* 1969;56:126-126.